iScience, Volume *26*

Supplemental information

Integrative systems biology characterizes immune-mediated neurodevelopmental changes in murine Zika virus microcephaly

Kimino Fujimura, Amanda J. Guise, Tojo Nakayama, Christoph N. Schlaffner, Anais Meziani, Mukesh Kumar, Long Cheng, Dylan J. Vaughan, Andrew Kodani, Simon Van Haren, Kenneth Parker, Ofer Levy, Ann F. Durbin, Irene Bosch, Lee Gehrke, Hanno Steen, Ganeshwaran H. Mochida, and Judith A. Steen

Figure S1

Intraplacental zika virus injection leads to smaller brain size of the embryos and induces elevated innate immune response. (Related to Figure 1A-F, 2C-D, 3A, 3H)

(A) Survival rates of embryos at E14.5 and E16.5. Box plot shows median, interquartile range, and maximum/minimum values.
(B) Brain weight in milligrams of Mock- or ZIKV-infected embryos at E16.5.
(C) Morphometric analysis of a representative E16.5 brain in 3 dimensions. Representative measurements of Mock-infected brain (lengths A-C) are overlaid on a representative ZIKV-infected brain.
(D) Measurements of lengths A-C expressed as percentage of lengths measured in Mock-infected brains.
(E) Virus copy number at E14.5 and E16.5 following intraplacental ZIKV or Mock infection at E10.5.
(F) Interaction network of proteins with strong positive correlation (Pearson correlation r > 0.90) with ZIKV polyprotein abundance. Node color indicates functional classification (red, catalytic activity; purple, catalytic and nucleotide-binding activities); edges represent high confidence interactions (confidence score = 0.70) between proteins in the network based on protein-protein interaction information curated by the STRING database; connected nodes are shown.
(G) Interaction network of proteins included in cluster 1-1 of **Figure 2C**. Node color indicates functional classification (yellow, innate immune response; light pink, antigen presentation, orange, both); edges represent high confidence interactions (confidence score = 0.70) between proteins based on in the network based on STRING database.
(H) Interaction network for the union of significantly increased-in-abundance and decreased-in-abundance RNA-proteins pairs. Node color indicates RNA-level fold change (log2(ZIKV/Mock)); edges represent high confidence interactions between nodes in the network based on protein-protein interaction information curated by the STRING database. Nodes outlined in blue indicate are associated with interferon signaling and innate immune response. Arrow-head node shape indicates association with neurogenesis and neurodevelopment.
(I) ClueGO network analysis of significantly increased-in-abundance RNA-protein pairs highlighting enriched immune-associated pathways (GO immune System Functional Pathway Database, EBI) network. Nodes indicate individual functional pathways. Node colors indicate interconnected pathways. Node size indicates significance of enrichment (p-value, Bonferroni step-down method) in the network. Edge width and transparency indicate kappa scores reflecting the similarity of genes associated with connected nodes.
Error bars indicate standard deviation.

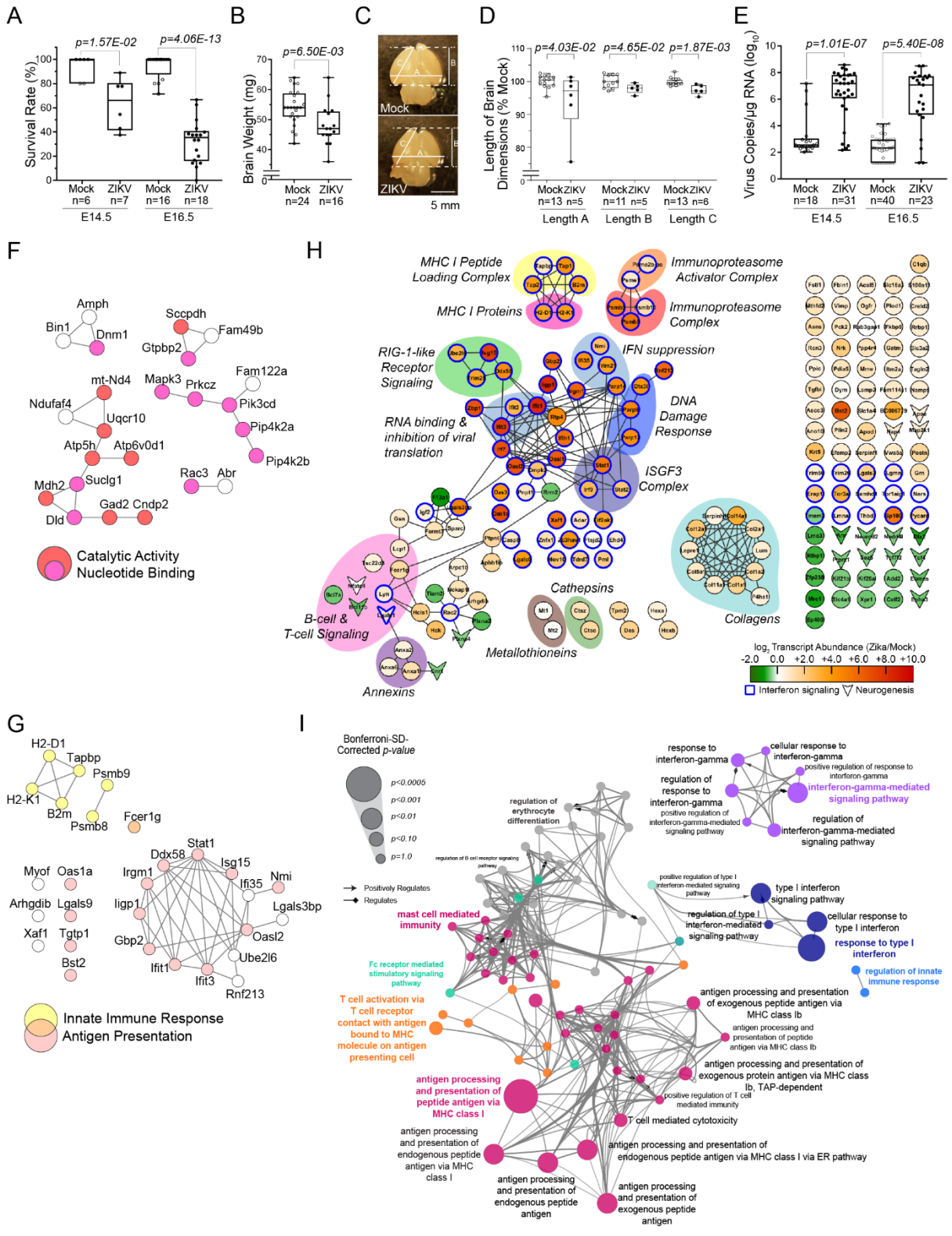
A
p=1.57E-02
p=4.06E-13
Survival Rate (%)
Mock n=6
ZIKV n=7
Mock n=16
ZIKV n=18
E14.5
E16.5
B
p=6.50E-03
Brain Weight (mg)
Mock n=24
ZIKV n=16
C
Mock
ZIKV
5 mm
D
p=4.03E-02
p=4.65E-02
p=1.87E-03
Length of Brain Dimensions (% Mock)
Mock n=13
ZIKV n=5
Mock n=11
ZIKV n=5
Mock n=13
ZIKV n=6
Length A
Length B
Length C
E
p=1.01E-07
p=5.40E-08
Virus Copies/µg RNA (log10)
Mock n=18
ZIKV n=31
Mock n=40
ZIKV n=23
E14.5
E16.5
F
Amph
Bin1
Dnm1
Sccpdh
Fam49b
Gtpbp2
mt-Nd4
Mapk3
Prkcz
Fam122a
Pik3cd
Ndufaf4
Uqcr10
Pip4k2a
Atp5h
Atp6v0d1
Pip4k2b
Rac3
Abr
Mdh2
Suclg1
Gad2
Cndp2
Dld
Catalytic Activity
Nucleotide Binding
H
MHC I Peptide Loading Complex
MHC I Proteins
Immunoproteasome Activator Complex
Immunoproteasome Complex
RIG-1-like Receptor Signaling
IFN suppression
RNA binding & inhibition of viral translation
DNA Damage Response
ISGF3 Complex
B-cell & T-cell Signaling
Cathepsins
Metallothioneins
Collagens
Annexins
log2 Transcript Abundance (Zika/Mock)
-2.0 0.0 +2.0 +4.0 +6.0 +8.0 +10.0
Interferon signaling
Neurogenesis
G
H2-D1
Tapbp
Psmb9
H2-K1
B2m
Psmb8
Fcer1g
Stat1
Ddx58
Isg15
Irgm1
Ifi35
Nmi
Myof
Oas1a
Lgals3bp
Arhgdib
Lgals9
Iigp1
Xaf1
Tgtp1
Gbp2
Oasl2
Bst2
Ube2l6
Ifit1
Ifit3
Rnf213
Innate Immune Response
Antigen Presentation
I
Bonferroni-SD-Corrected p-value
p<0.0005
p<0.001
p<0.01
p<0.10
p=1.0
Positively Regulates
Regulates
response to interferon-gamma
cellular response to interferon-gamma
positive regulation of response to interferon-gamma
regulation of response to interferon-gamma
interferon-gamma-mediated signaling pathway
positive regulation of interferon-gamma-mediated signaling pathway
regulation of interferon-gamma-mediated signaling pathway
regulation of erythrocyte differentiation
positive regulation of type I interferon-mediated signaling pathway
type I interferon signaling pathway
regulation of type I interferon-mediated signaling pathway
cellular response to type I interferon
response to type I interferon
regulation of innate immune response
mast cell mediated immunity
Fc receptor mediated stimulatory signaling pathway
T cell activation via T cell receptor contact with antigen bound to MHC molecule on antigen presenting cell
antigen processing and presentation of exogenous peptide antigen via MHC class Ib
antigen processing and presentation of peptide antigen via MHC class Ib
antigen processing and presentation of exogenous protein antigen via MHC class Ib, TAP-dependent
antigen processing and presentation of peptide antigen via MHC class I
positive regulation of T cell mediated immunity
T cell mediated cytotoxicity
antigen processing and presentation of endogenous peptide antigen via MHC class I
antigen processing and presentation of endogenous peptide antigen via MHC class I via ER pathway
antigen processing and presentation of endogenous peptide antigen
antigen processing and presentation of exogenous peptide antigen

Figure S2

Congenital ZIKV infection activates the interferon-induced pathways in the embryonic brain. (Related to Figure 3A-F)

Significant transcript expression changes ($q < 0.05$) mapped to interferon-induced pathways based on pathway analysis conducted by QIAGEN Ingenuity Pathway Analysis. Node shape represents the function of the edges; solid line, direct interaction; dashed line, indirect interaction; red, upregulated transcripts; grey, no significant changes.

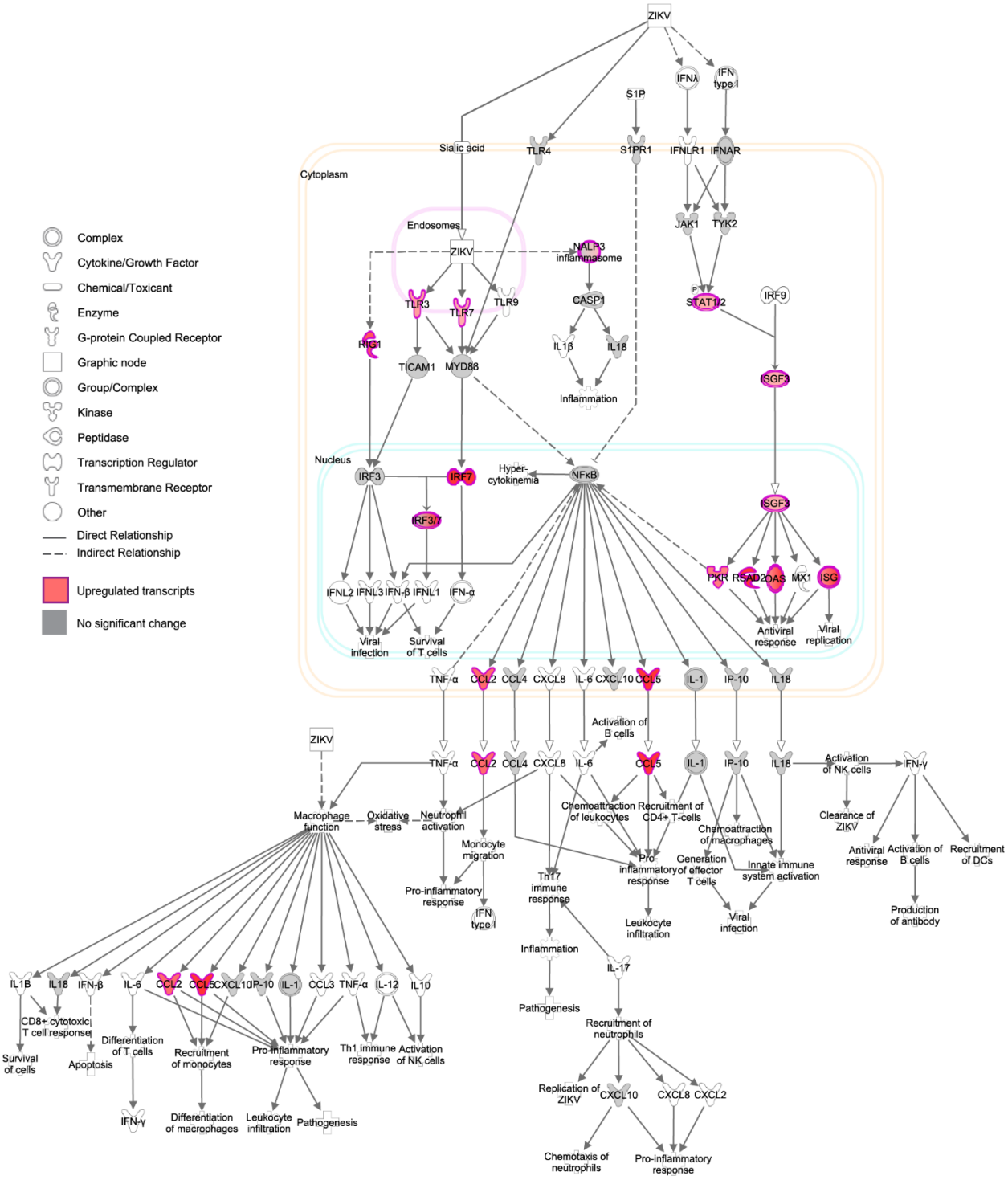
Complex
Cytokine/Growth Factor
Chemical/Toxicant
Enzyme
G-protein Coupled Receptor
Graphic node
Group/Complex
Kinase
Peptidase
Transcription Regulator
Transmembrane Receptor
Other
Direct Relationship
Indirect Relationship
Upregulated transcripts
No significant change
ZIKV
IFNλ
IFN type I
S1P
Sialic acid
TLR4
S1PR1
IFNLR1
IFNAR
Cytoplasm
JAK1
TYK2
Endosomes
ZIKV
NALP3 inflammasome
TLR3
TLR7
TLR9
CASP1
STAT1/2
IRF9
RIG-I
IL1β
IL18
TICAM1
MYD88
ISGF3
Inflammation
Nucleus
IRF3
IRF7
Hyper-cytokinemia
NFκB
IRF3/7
ISGF3
IFNL2
IFNL3
IFN-β
IFNL1
IFN-α
PKR
RSAD2
OAS
MX1
ISG
Viral infection
Survival of T cells
Antiviral response
Viral replication
TNF-α
CCL2
CCL4
CXCL8
IL-6
CXCL10
CCL5
IL-1
IP-10
IL18
ZIKV
Activation of B cells
TNF-α
CCL2
CCL4
CXCL8
IL-6
CCL5
IL-1
IP-10
IL18
Activation of NK cells
IFN-γ
Macrophage function
Oxidative stress
Neutrophil activation
Chemoattraction of leukocytes
Recruitment of CD4+ T-cells
Chemoattraction of macrophages
Clearance of ZIKV
Monocyte migration
Pro-inflammatory response
Generation of effector T cells
Innate immune system activation
Antiviral response
Activation of B cells
Recruitment of DCs
Th17 immune response
Pro-inflammatory response
IFN type I
Leukocyte infiltration
Viral infection
Production of antibody
Inflammation
IL-17
IL1B
IL18
IFN-β
IL-6
CCL2
CCL5
CXCL10
IP-10
IL-1
CCL3
TNF-α
IL-12
IL10
Pathogenesis
CD8+ cytotoxic T cell response
Differentiation of T cells
Recruitment of monocytes
Pro-inflammatory response
Th1 immune response
Activation of NK cells
Recruitment of neutrophils
Survival of cells
Apoptosis
IFN-γ
Differentiation of macrophages
Leukocyte infiltration
Pathogenesis
Replication of ZIKV
CXCL10
CXCL8
CXCL2
Chemotaxis of neutrophils
Pro-inflammatory response

Figure S3

Immunohistochemistry staining results show activation of antigen presentation pathways, recruitment of macrophages/microglia, and induction of apoptosis after ZIKV infection. (Related to Figure 3D-E)

(A) Immunohistochemistry (IHC) staining of cortices of Mock- or ZIKV-infected E14.5 brains with proteasome 20S Subunit Beta 9 (PSMB9) (green), MHC-I (red), and Hoechst 33342 (nucleus, blue). CP, cortical plate; IZ, intermediate zone; VZ, ventricular zone; SVZ, subventricular zone. Scale bar = 50 μm.

(B) IHC staining of cells in the E14.5 CP of Mock- or ZIKV-infected brains stained for PSMB8 (green), MHC-I (red), ZIKV (purple), and Hoechst (nucleus, blue). Scale bar = 10 μm.

(C) IHC staining of the VZ/SVZ, IZ, and CP of Mock- or ZIKV-infected E14.5 brains stained for allograft inflammatory factor 1 (IBA1) (green), MHC-I (red), and Hoechst (nucleus, blue).

(D) Higher magnification of the sections indicated by the dotted square in 3F. Triangles, MHC-I-presenting neural cells; arrows, cells with overlapping signals of IBA1 and MHC-I, suggesting the engulfment of MHC-I-presenting cells by macrophage/microglia. Note that the IBA-positive cells are located adjacent to the endothelial cells of blood vessels, indicated by asterisks. Scale bar = 20 μm.

(E) IHC staining of Mock-or ZIKV-infected E16.5 brains with Cleaved Caspase 3 (Cl-Casp3) (red), ZIKV (green), and Hoechst (nucleus, blue), scale bar = 100 μm.

(F) Higher magnification of **D** of the ZIKV-infected brain, scale bar = 10μm.

(G) Quantification of cleaved caspase 3 (Cl-Casp3)-positive cells per unit area in Mock-or ZIKV-infected embryonic brains. Mock, n = 7 from 7 litters; zika, n = 7 from 6 litters. Error bars indicate standard deviation.

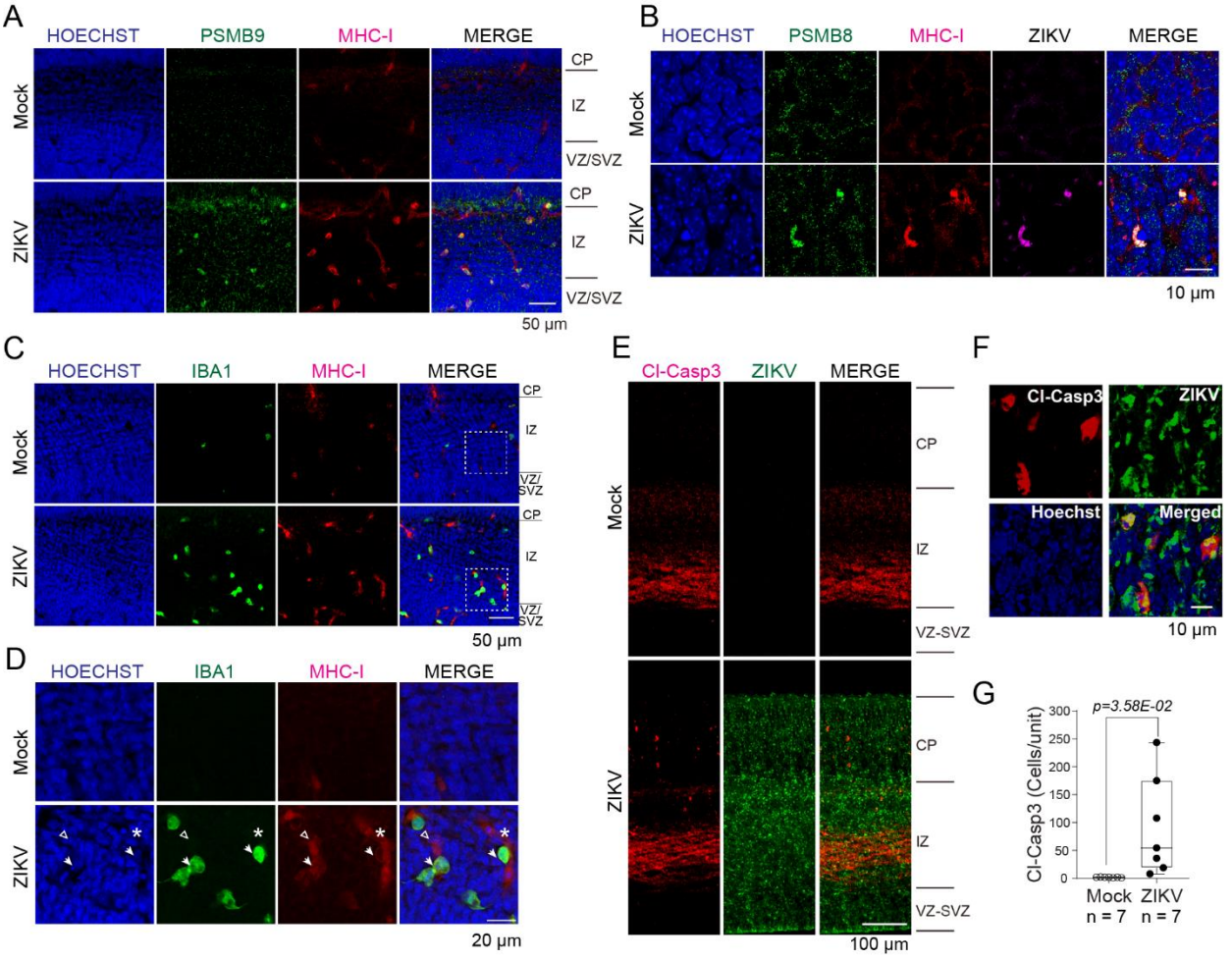

Figure S4

ZIKV infection downregulates neurodevelopmental genes/proteins leading to diminished numbers of neurons in the cortical plate. (Related to Figure 3G)

Interaction network for the protein-RNA pairs that did not match with respect to the changes in abundance (Quadrant II and IV of **Figure 3G**). Node color represents the function of the proteins (light blue, neurodevelopmental genes; purple, cell cycle; green, cell adhesion; peach, collagen and cell adhesion); edges represent high confidence interactions (confidence score = 0.70) between proteins in the network based on protein-protein interaction information curated by the STRING database.

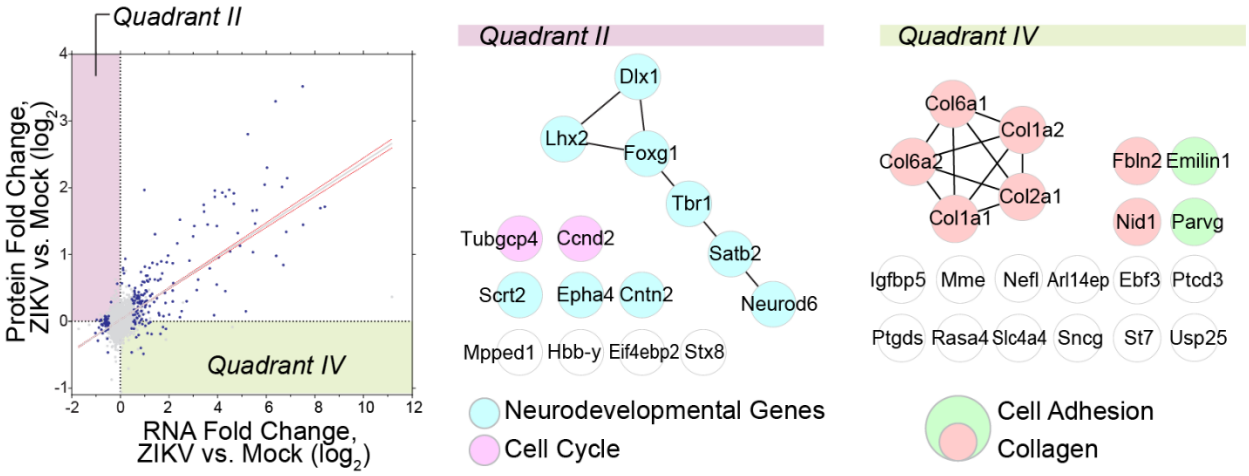

Table S7

Downregulated protein-transcript pairs reported to have neurodevelopmental functions *(Related to Figure 4A)*

Mouse gene symbol	Neurodevelopmental functions
Dlx2	Terminal differentiation of interneurons; development of ventral forebrain [95, 96, 97, 98]
Ep400	Survival of the oligodendrocytes and myelination in the vertebrate central nervous system [99]
Kif26a	Repression of cell growth signaling pathway during enteric nervous system development [100]
Plxna4	Axon guidance and migration of sympathetic neurons [101]
Ptprz1	Inhibition of proliferation and promotion of maturation of oligodendrocytes; establishment of contextual memory [102, 103]
Sez6	Dendrite elongation and branching and excitatory synapse formation of the cerebral cortical neurons [104]
Tiam2	Neurite growth and growth cone remodeling of the hippocampal neurons; migration of cerebral cortical neurons [105, 106]

.

Supplemental References *(Related to Table S7)*

95. Porteus, M.H., Bulfone, A., Ciaranello, R.D., and Rubenstein, J.L. (1991). Isolation and characterization of a novel cDNA clone encoding a homeodomain that is developmentally regulated in the ventral forebrain. Neuron *7*, 221-229. 10.1016/0896-6273(91)90260-7.
96. Anderson, S.A., Eisenstat, D.D., Shi, L., and Rubenstein, J.L. (1997). Interneuron migration from basal forebrain to neocortex: dependence on Dlx genes. Science *278*, 474-476.
97. Colasante, G., Collombat, P., Raimondi, V., Bonanomi, D., Ferrai, C., Maira, M., Yoshikawa, K., Mansouri, A., Valtorta, F., Rubenstein, J.L., and Broccoli, V. (2008). Arx is a direct target of Dlx2 and thereby contributes to the tangential migration of GABAergic interneurons. J Neurosci *28*, 10674-10686. 10.1523/JNEUROSCI.1283-08.2008.
98. Feng, L., Eisenstat, D.D., Chiba, S., Ishizaki, Y., Gan, L., and Shibasaki, K. (2011). Brn-3b inhibits generation of amacrine cells by binding to and negatively regulating DLX1/2 in developing retina. Neuroscience *195*, 9-20. 10.1016/j.neuroscience.2011.08.015.
99. Elsesser, O., Frob, F., Kuspert, M., Tamm, E.R., Fujii, T., Fukunaga, R., and Wegner, M. (2019). Chromatin remodeler Ep400 ensures oligodendrocyte survival and is required for myelination in the vertebrate central nervous system. Nucleic Acids Res *47*, 6208-6224. 10.1093/nar/gkz376.
100. Zhou, R., Niwa, S., Homma, N., Takei, Y., and Hirokawa, N. (2009). KIF26A is an unconventional kinesin and regulates GDNF-Ret signaling in enteric neuronal development. Cell *139*, 802-813. 10.1016/j.cell.2009.10.023.
101. Waimey, K.E., Huang, P.H., Chen, M., and Cheng, H.J. (2008). Plexin-A3 and plexin-A4 restrict the migration of sympathetic neurons but not their neural crest precursors. Dev Biol *315*, 448-458. 10.1016/j.ydbio.2008.01.002.
102. Tamura, H., Fukada, M., Fujikawa, A., and Noda, M. (2006). Protein tyrosine phosphatase receptor type Z is involved in hippocampus-dependent memory formation through dephosphorylation at Y1105 on p190 RhoGAP. Neurosci Lett *399*, 33-38. 10.1016/j.neulet.2006.01.045.
103. Lamprianou, S., Chatzopoulou, E., Thomas, J.L., Bouyain, S., and Harroch, S. (2011). A complex between contactin-1 and the protein tyrosine phosphatase PTPRZ controls the development of oligodendrocyte precursor cells. Proc Natl Acad Sci U S A *108*, 17498-17503. 10.1073/pnas.1108774108.
104. Gunnersen, J.M., Kim, M.H., Fuller, S.J., De Silva, M., Britto, J.M., Hammond, V.E., Davies, P.J., Petrou, S., Faber, E.S., Sah, P., and Tan, S.S. (2007). Sez-6 proteins affect dendritic arborization patterns and excitability of cortical pyramidal neurons. Neuron *56*, 621-639. 10.1016/j.neuron.2007.09.018.
105. Kawauchi, T., Chihama, K., Nabeshima, Y., and Hoshino, M. (2003). The in vivo roles of STEF/Tiam1, Rac1 and JNK in cortical neuronal migration. EMBO J *22*, 4190-4201. 10.1093/emboj/cdg413.
106. Matsuo, N., Terao, M., Nabeshima, Y., and Hoshino, M. (2003). Roles of STEF/Tiam1, guanine nucleotide exchange factors for Rac1, in regulation of growth cone morphology. Mol Cell Neurosci *24*, 69-81. 10.1016/s1044-7431(03)00122-2.